IEEE Access
Multidisciplinary | Rapid Review | Open Access Journal

Received July 9, 2018, accepted August 13, 2018, date of publication September 24, 2018, date of current version October 25, 2018.

Digital Object Identifier 10.1109/ACCESS.2018.2868702

Embedded Sensors in Coastal Structures for On-Site Wave Impact Pressure Monitoring

FRANCK LUTHON[1,2], (Senior Member, IEEE), DORIAN D'AMICO[2], AND BENOÎT LARROQUE[1,3]

[1]IUT Bayonne Institute of Technology, Université de Pau et des Pays de l'Adour/E2S UPPA, 64600 Anglet, France
[2]LIUPPA-MIRA Computer Science Laboratory, E2S UPPA, 64600 Anglet, France
[3]SIAME Engineering Sciences Laboratory, Université de Pau et des Pays de l'Adour, 64600 Anglet, France

Corresponding author: Franck Luthon (franck.luthon@univ-pau.fr)

This work was supported in part by the Basque Country Urban Agglomeration CAPB and in part by the Research Federation on Aquatic Resources MIRA under Grant 1-2017-56.

ABSTRACT The climate change induces heavy storms that impact coastal environments. In order to predict such events or to adapt coastal structures in the future, it is desirable to be able to monitor the action of waves. Thanks to new technologies, one can embed sensors on dykes and have access remotely and continuously to field data measurements. In this paper, an *in situ* system, installed in September 2014, to measure the wave impact pressure is described. Additionally, the preliminary results of data processing are given.

INDEX TERMS Breakwater, dyke, environmental variable, field data, pressure sensor, seawall, signal processing.

I. INTRODUCTION

The supervision of the impact of waves on coastal structures has been a subject of research for a long time. De Rouville *et al.* [1] in 1938 was one of the first specialists to deal extensively with the use of sensors embedded in dykes to acquire field data measurements of the pressure, height and velocity of water. His work was part of an International Commission starting in 1927 involving countries having many sea borders such as: France, Great-Britain, Italy, Spain and Chile. He pointed out the variability of the signals, the difference between swell and breakers, the influence of the air trapped within breaking waves, the need to acquire data continuously in time, densely in space, and with a low time constant and high sampling frequency, the advantages of piezoelectric pressure sensors that have a high normal frequency ($>1\ kHz$). He also mentioned the use of photography or cinematography to correlate recorded data with wave profiles, explaining that the proportion of interesting records was never more than 5%, due to the complexity of the phenomenon (interaction between successive waves, interaction with ground depth, influence of wind etc.), not to mention the difficulty of installing a system in a very adverse environment. His records give some typical values for high pressure ($70\ \text{tons}/m^2 = 7$ bar), short duration (5 ms), water speed (horizontal: 10 m/s, vertical: 30 m/s), wavelength (40 m), acceleration (20 cm/s/s).

In 1939, Bagnold [2] complemented the full-scale work of De Rouville with laboratory work in a model wave-tank.

Since then, many works have been done about the mechanical study and the nature of the various wave types, the *in-situ* measurement of impacts, or the theoretical modeling of interactions between waves and structures. A mathematical model is proposed in [3] where the pressure impulse I_P (integral of pressure over time) and the rise time t_r are used to infer the maximum peak pressure P_k. In 1998, Bird *et al.* [4] present new transducers to measure both impact pressure and seawater aeration. The instrumentation is deployed in a test site in the English Channel, enabling full scale studies.

More recently, large scale experiments in an artificial flume with a vertical wall were conducted by Kaminski and Bogaert [5] and Hofland *et al.* [6]. A high spatial and temporal resolution is achieved, and four types of impact profiles are classified: slosh impact, flip through impact, air pocket impact and aerated impact (Fig. 1).

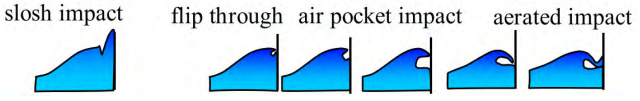

FIGURE 1. Wave profiles with increasing air pocket size (reprint from [6]).

They insist on the non-repeatability of the phenomena even in a controlled situation, and hence the need of

stochastic analysis. They show the four typical pressure time-series that can be obtained in the artificial flume. The flip-through impact yields the highest pressures with short rise times. Sloshing gives small pressure with long durations. The oscillations in the signals indicate the presence of air content, the higher the oscillation frequency, the smaller the entrapped air. Numerical modeling of flip-through impact is compared to experimental data in [7].

II. SITE LOCATION AND INSTRUMENTATION SETUP

The coastal structure under study is the Artha dyke in the bay of Saint-Jean de Luz in the south of France along the Atlantic ocean. The site location is given in the map of Fig. 2. A picture of the seawall is shown in Fig. 3, where the electrical enclosure and photovoltaic panel are visible.

FIGURE 2. Location of the Artha dyke in north Atlantic ocean (43.3985°N, 1.6745°W).

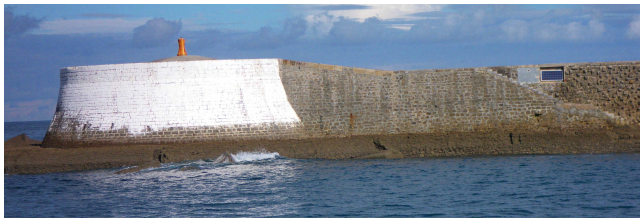

FIGURE 3. The dyke (view of the protected side) with electrical instrumentation setup on the right.

A. PRESSURE SENSORS

Two pressure sensors are embedded in the wall, separated by a vertical distance of 1.90 m (Fig. 4a). The wall is 4.60 m high, the lower sensor being at 1.10 m above the bottom level of the berm. The upper sensor is never below the sea level, whereas the lower sensor (Fig. 4b) might be below the sea level, depending on tidal conditions: for the highest tides, it is about 10 to 20 cm below the sea-level.

The type of sensor is piezoresistive absolute pressure transmitter (reference Keller© PAA-25). Table 1 gives the main characteristics of the sensors.

a) b)

FIGURE 4. a) Two pressure sensors embedded in the seawall; b) Close view of the lower sensor at installation time (late 2014) and 3 years later (mid 2017).

TABLE 1. Pressure sensor specifications.

Specification	Value
signal output/Type	4...20mA /2-Wire
frequency response	1 kHz
range (FS=full scale)	0-5 bar for lower sensor
range (FS)	0-10 bar for upper sensor
typical error	±0.2% FS
protection	IP68

a) b)

FIGURE 5. Hostile environmental conditions at Artha dyke: a) huge breaking wave during a storm; b) block of 50 tons lifted up by the waves and dropped off on the seawall during a storm in March 2017.

Despite the hostile environment (Fig. 5), the installation worked continuously for more than 2 years.

B. ACQUISITION SYSTEM

As the Artha dyke is an offshore isolated site (no power grid available on-site), it was necessary to install an autonomous system both energetically and communication prone. Fig. 6 gives the schematic diagram of the complete system and Fig. 7 illustrates the electrical setup enclosed in the protected side of the seawall.

It consists of three main parts: (i) power supply, (ii) sensor data acquisition, and (iii) data transmission. To supply the electrical energy required for acquisition and transmission, a photovoltaic system is installed on the seawall. The power supply consists of three components: photovoltaic panel (SolarWorld© 150Wp), solar charge controller (Steca Solarix© PRS 1010 12/24V 10A) and high capacity

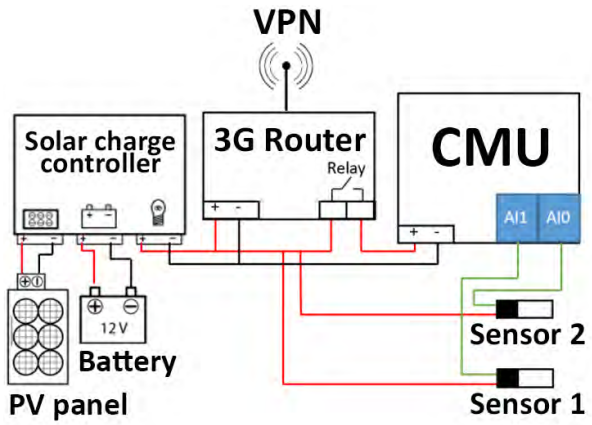

FIGURE 6. Instrumentation setup for autonomous data acquisition and transmission (CMU: Central Measurement Unit; VPN: Virtual Private Network; PV: Photovoltaic panel).

FIGURE 7. Photograph of the electrical setup embedded in the seawall.

battery (Banner© SBV 200 -12V 200Ah). For wireless communication, a 3G router (UR5i v2, 3G UMTS/HSPA) and a virtual private network (VPN) are configured to ensure a reliable communication channel with the data acquisition system (remote parameter setting, measurement readings and data transmission). Moreover, since weather conditions are extreme during storm periods, the instrumentation equipment is selected accordingly for robustness and flexibility. For that purpose, a CompactRIO 9076 from National Instruments© is used as the core of the central measurement unit, with many advantages: embedded control, rugged package, modular acquisition, linux embedded system (with webserver), high storage memory, and FPGA based board (high sampling rate). It controls four DAQ acquisition modules NI 9203 (8-Channel, analog inputs ±20mA, 16-bit resolution) so that a total of 32 sensors can be plugged (here, only two of them are used).

C. ADDITIONAL ENVIRONMENTAL DATA

In addition to the pressure sensors, the swell motion (in the 3 directions x, y, z) is recorded at a sampling frequency of 1.28 Hz, thanks to a wave-buoy located 1.25 km away in the ocean (data available by courtesy of Candhis national center: candhis.cetmef.developpement-durable.gouv.fr/). A sample record during 400 s is shown in Fig. 8b. The wave period T_w and other parameters are available from those records, such as the $H_{1/10}$ value, which is the average value of the 10% of highest vertical amplitudes of swell registered during 30 min.

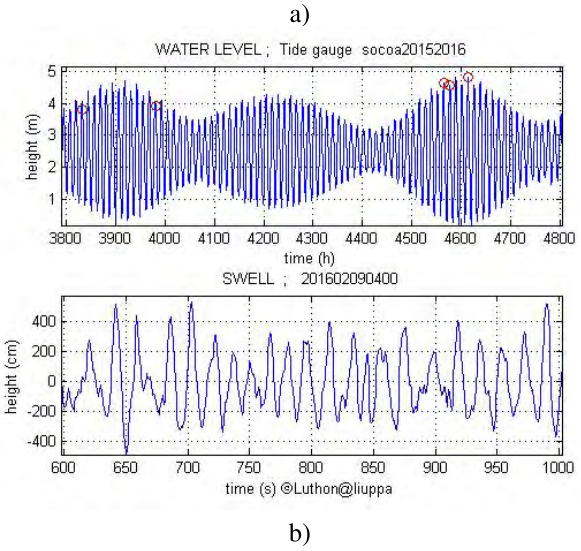

FIGURE 8. a) Sea level records during 45 days (≈1000 hours); b) Vertical amplitude of swell recorded for 400s.

Moreover, a tide gauge located in Socoa Fort just near the dyke (see location on the left in Fig. 2) gives the sea level every hour, recorded during 8 months from September 2015 to April 2016. A sample is shown in Fig. 8a.

Finally, a meteorological station near the dyke gives information about the wind velocity and direction, acquired at a sampling frequency of about 0.33 Hz and recorded after averaging every 10 min, from Sept. 2015 to March 2016 (during 7 months). As shown in Fig. 9, the wind comes mainly from West-Northwest (270°) and its maximal speed is 22 m/s (80 km/h).

Those environmental data will be correlated with wave impact pressures registered at the seawall in our future ongoing research. The ideal objective (maybe unrealistic) is indeed to infer the maximal pressures by prediction from those data. To that end, a 3D-model of wave propagation is currently under investigation by our colleagues specialists in hydrodynamics applied to coastal engineering.

A preliminary statistical analysis [8] indicates that peak pressure variability is mainly explained by wave height, then by water level, somewhat by wave period, but not at all by local wind. Of course those first results obtained from ANOVA tests deserve more validation.

III. SIGNAL PROCESSING

Wave impact pressure is acquired 24/24 and 7/7 at a sampling frequency of $F_s = 10\ kHz$, during 10 min every hour.

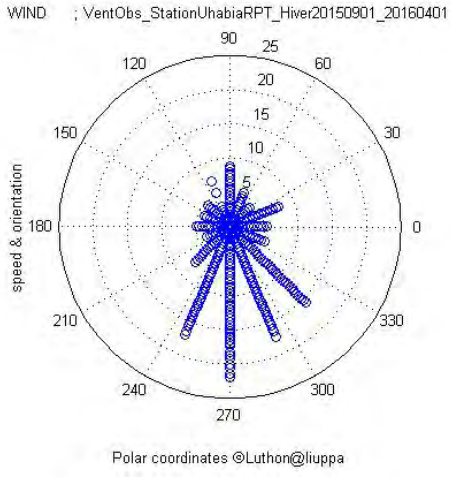

FIGURE 9. Wind distribution during 7 months experiment.

A typical 10 min acquisition of the two sensors during a storm period is shown in Fig. 10a. A zoom of the impacts after scaling and filtering is shown in Fig. 10b.

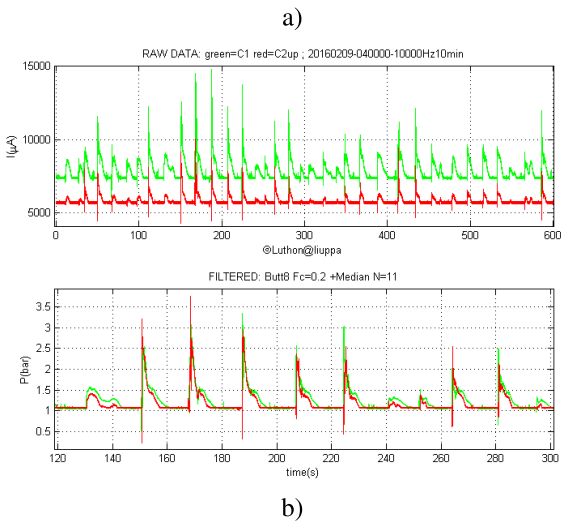

FIGURE 10. a) Raw data (in μA) recorded by lower (green curve) and upper (red curve) sensors; b) zoom on impact signals, after scaling (in bar) and filtering.

Scaling consists in converting the current I in μA into pressure P in bar, following the linear calibration equation:

$$P = P_{max}\frac{I - 4000}{20000 - 4000}, \tag{1}$$

where P_{max} is the dynamic range of the sensor (5 or 10 bar depending on the sensor).

Filtering consists of a median filter ($N = 11$) combined with a Butterworth low-pass filter of order 8 (cut-off frequency $F_c = 1\ kHz$). First, the non-linear median filter eliminates isolated values due to noise or erroneous pressure levels lasting less than 5 consecutive sampling points acquired at $F_s = 10\ kHz$. Indeed, they correspond to changes that are too short for being relevant (the median filter does not smooth significant variations lasting more than 0.5 ms). Then the linear low-pass filter eliminates all frequencies higher than the normal frequency of the sensor ($F_n = 1\ kHz$); of course, it also smoothes a bit the signal variations around its cut-off frequency.

Worth mentioning is the fact that among all the pressure time-series recorded during 5 months between Nov. 2015 and April 2016 (3797 records of 10 min), less than 20% of the data (611 records) contain significant wave impacts on the lower sensor, and only 20% of those records also contain impacts on the upper sensor (125 records), meaning that less than 4% of all the records imply the upper sensor. Indeed, only at high tides or during storms are the sensors impacted, otherwise, they just measure the atmospheric pressure. In this experimental setup, the lower sensor was purposely installed at the upper limit of high tides (see red circles superimposed on Fig. 8a, pointing out typical instants where rare flip-through impacts are registered: it always occurs at high tides).

One first outcome of this full scale experiment is that, just before wave impacts, a short under-pressure often appears in the signals, as shown in Fig. 10b where the pressure falls below the atmospheric value of 1 bar. To the best of our knowledge, this fact has never been noticed before, even though this phenomenon was already visible in a result sample presented in [4].

One can compute the covariance $C(\tau)$ between upper and lower sensor signals (Fig. 11): the time instant τ corresponding to its maximum leads to a precise estimate of the delay d of impact between both sensors. This information might help to classify impact profiles.

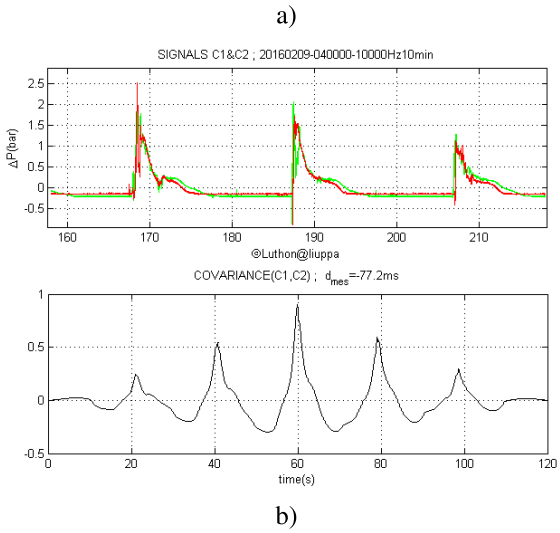

FIGURE 11. a) A slice of 1 minute of the pressure signals from the two sensors; b) Covariance computed from those signals, with estimated delay d_{mes}.

Note that in Fig. 11 and the following ones, the relative pressure $\Delta P = P - P_{init}$ is graphed instead of P, where P_{init} is the static pressure (typ. atmospheric pressure) as only variations are relevant.

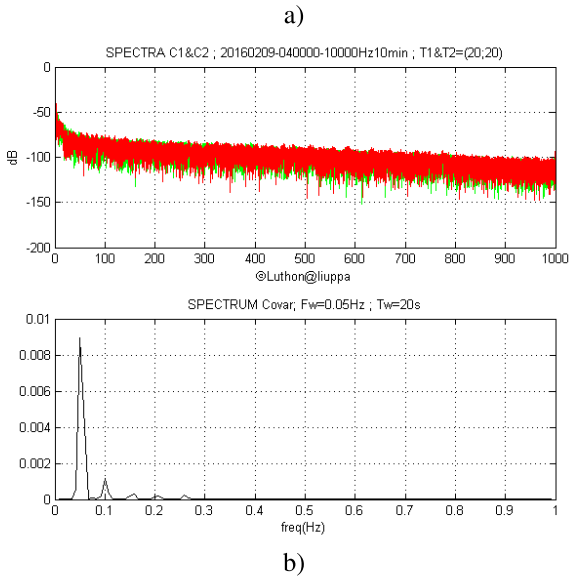

FIGURE 12. **a) Spectrum of the signals (in the range 0-1 kHz); b) Spectrum of the Covariance (zoom in the range 0-1 Hz) leading to estimation of wave period T_W (on 1 minute signals).**

The Fourier transform of the covariance gives the power spectral density of the signals (Fig. 12). The main peak exhibited in the low-frequency range indicates the wave impact frequency (here $F_w = 0.05\ Hz$). This yields automatically to the wave impact period $T_w = \frac{1}{F_w}$. This value can be compared to and is indeed highly correlated with the wave period measured by the off-shore wave-buoy.

A classification of the four types of impacts (listed in section I) based on the acquired waveforms is under study.

The oscillations after the impact can be measured with their period (as low as 15 ms for near flip-through impact, and about 400 ms for air-pocket impact); they supposedly correspond to the presence of air entrapped in water [5].

A typical flip-through waveform is visible in the sequence of Fig. 13 around time $t = 200\ s$.

The impact is quick (rise time $t_r \approx 20ms$), followed by fast oscillations ($T_{osc} \approx 100ms$) and by a long-lasting tail ($D \approx 2\ s$). Impulse integral is small $I_P \approx 0.6$. Note that flip-through impact is infrequent (less than 1% of the cases). In our experiment, it occurs only at high tides: the red circles in Fig. 8a indicate the times where some of the flip-through impacts were recorded. Unlike [6], flip-through peak pressures are not as big as those obtained in artificial channels (4 bar max instead of 20 bar). This remark has already been reported in [2].

Air pocket impact is shown in Fig. 14. The impact is longer ($D \approx 5s$), rise time is longer, and there are oscillations with lower frequency than flip-through (typ. period of $T_{osc} = 400ms$). The pressure impulse integral I_P is much bigger than for flip-through impact.

Aerated impact is shown in Fig. 15. The pressure peak is much lower, the rise time is bigger. It lasts a long time ($D \approx 8s$). Those impacts happen very often.

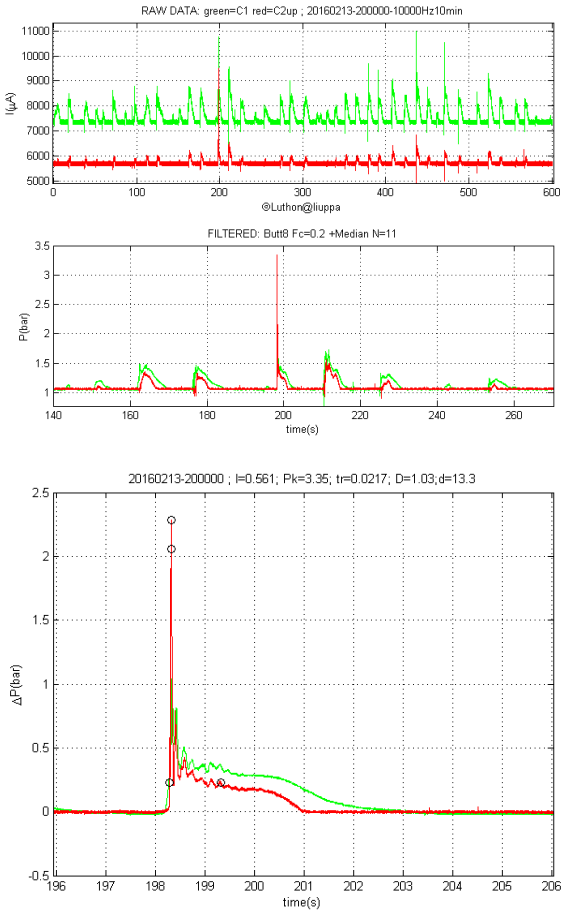

FIGURE 13. **Typical flip-through impact occuring on upper sensor at $t \approx 200s$.**

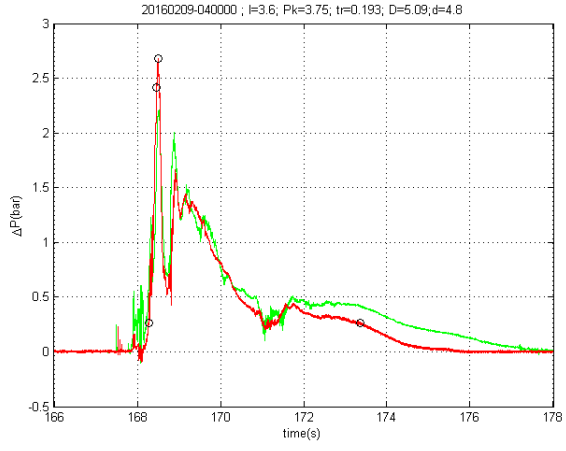

FIGURE 14. **Air pocket impact pressure signal.**

Slosh impact is visible in Fig. 16. Rising is slow ($t_r > 1s$), there is no oscillation and it lasts a long time ($D \approx 6s$). Pressure peak is low. Impulse integral I_P is not so big.

A statistical analysis with computation of Pearson cœfficient r for about 100 impacts with high peaks yields the following preliminary results:

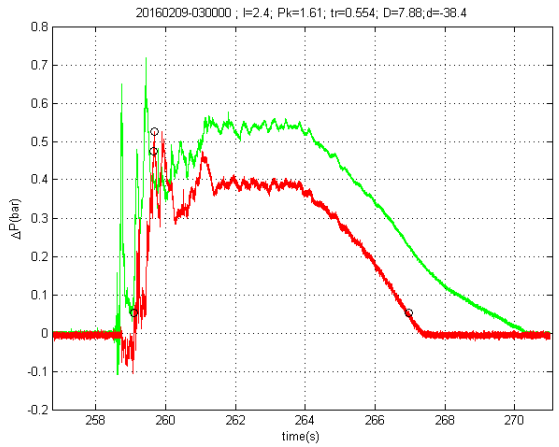

FIGURE 15. Aerated impact pressure signal.

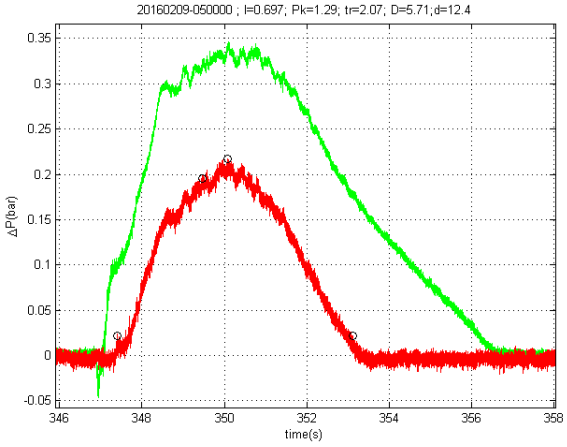

FIGURE 16. Slosh impact pressure signal.

- there is a strong positive correlation ($r > 60\%$) between pressure impulse integral I_P and maximal amplitude of pressure peak P_k,
- there is a strong positive correlation ($r > 50\%$) between rise time t_r and impact duration D,
- there is a positive correlation ($r \approx 40\%$) between wave period T_w and P_k,
- there is a negative correlation between t_r and P_k.

TABLE 2. Typical wave impact parameters.

Impact type	P_k (bar)	t_r	D (s)	I_P	T_{osc} (ms)
Flip through	> 3	$10 - 50ms$	2	< 1	15-100
Air Pocket	2.5-3.5	$250ms$	5-6	3	200-500
Aerated	1.5-2	$0.5 - 1s$	6-9	2	300
Slosh	< 1.5	$> 1s$	5-9	< 1	-
Minima	0.2	$1ms$	0.2	0.1	15
Maxima	4	$2.3s$	10	4	500

The typical values listed in Table 2 give orders of magnitude of the various parameters. They are measured automatically on chosen impacts. Note that we do not claim that those values have more significance than simply illustrating what we obtain in this full scale experiment. Some trends are in agreement with what was reported in the literature, but some results are specific to our configuration for study.

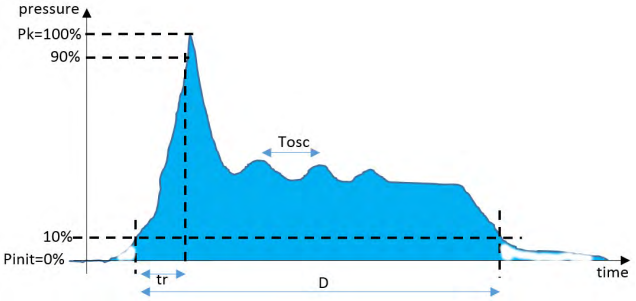

FIGURE 17. Pressure impulse parameters.

The rise time t_r is computed as the time difference to rise from 10% to 90% of the maximal pressure P_k, starting from initial (atmospheric) pressure P_{init}. The duration D is the time during which the impact signal remains above 10% of P_k. Possibly, the period of oscillations T_{osc} is also measured, when the signal oscillates a few times while decreasing after its maximum value. The integral I_P is computed as the surface under the curve during the temporal interval D. Fig. 17 illustrates all those pressure impulse parameters.

IV. CONCLUSION

The correlation between pressures and other environmental data is under investigation. Our first results indicate that there is a strong correlation between peak pressure P_k and maximal vertical swell value $H_{1/10}$. In order to conduct exhaustive analysis of wave impacts, a bigdata platform will be used with machine learning facilities, thanks to an industrial partnership with the HUPI company, Bidart, France.

As regards perspectives, a camera will be installed on the top of the Socoa Fort just near the dyke, to visualize from profile the wave shapes in addition to the recording of impact pressures.

In autumn 2018, a network of 22 sensors will be embedded in the seawall, to get 2D spatial information about wave impacts, instead of only 1D vertical information as shown in the current study.

ACKNOWLEDGMENT

The authors would like to thank the Communauté d'Agglomération du Pays Basque and the MIRA research federation (FED 4155) for joint funding of PhD grant of Dorian d'Amico, and the Council of Département64 for civil engineering work, installation and maintenance of the sensors in the seawall. They are also grateful to Stéphane Abadie for his expertise in coastal engineering, to Pierre-Antoine Poncet and Benoît Liquet for fruitful discussions, and to Philippe Arnould for his contribution in network configuration of the wireless communication system. Finally, they thank Gisèle Sigal for her help in correcting English flaws in the manuscript.

REFERENCES

[1] M. A. De Rouville, P. Besson, and P. Petry, "Etat actuel des études internationales sur les efforts dus aux lames," *Ann. Ponts Chaussées*, vol. 108, pp. 5–113, Jul. 1938.
[2] R. A. Bagnold, "Interim report on wave-pressure research," *Eng. Res.*, vol. 12, pp. 201–226, Jun. 1939.
[3] M. J. Cooker and D. H. Peregrine, "A model for breaking wave impact pressures," in *Proc. 22nd Int. Conf. Coastal Eng.*, 1990, pp. 1473–1486.
[4] P. A. D. Bird, A. R. Crawford, P. J. Hewson, and G. N. Bullock, "An instrument for field measurement of wave impact pressures and seawater aeration," *Coastal Eng.*, vol. 35, pp. 103–122, Oct. 1998.
[5] M. L. Kaminski and H. Bogaert, "Full scale sloshing impact tests," in *Proc. 19th Int. Polar Eng. Conf.*, Osaka, Japan, Jun. 2009, pp. 125–134.
[6] B. Hofland, M. L. Kaminski, and G. Wolters, "Large scale wave impacts on vertical wall," in *Proc. Coastal Eng.*, 2010, pp. 1–15.
[7] H. Bredmose, A. Hunt-Raby, R. Jayaratne, and G. N. Bullock, "The ideal flip-through impact: Experimental and numerical investigation," *J. Eng. Math.*, vol. 67, pp. 115–136, Jun. 2010.
[8] B. Larroque, P. Arnould, F. Luthon, P. A. Poncet, A. Rahali, and S. Abadie, "*In-situ* measurements of wave impact pressure on a composite breakwater: Preliminary results," *J. Coastal Res., Coastal Educ. Res. Found.*, no. 85, pp. 1086–1090, 2018.

FRANCK LUTHON (M'01–SM'08) received the engineer's degree in electronics and the Ph.D. degree from the National Polytechnical Institute INP, Grenoble, France, in 1985 and 1988, respectively. He was an Assistant Professor with the National Polytechnical Institute INP for ten years. Since 2000, he has been a Professor with the Université de Pau et des Pays de l'Adour, Bayonne, France. He was the Founder and the Head of the Industrial Engineering Department, Technical University Institute IUT, Anglet, France. His fields of interest are signal and image processing, electronic systems, and learning technologies.

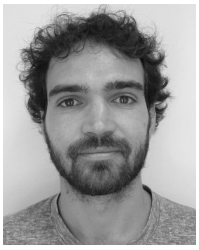

DORIAN D'AMICO received the master's degree in computer science and telecommunications from the University Paul Sabatier, Toulouse, France, in 2016. He is currently pursuing the Ph.D. degree with the Computer Engineering Lab, Université de Pau et des Pays de l'Adour, Anglet, France. His field of research is big data applied to the supervision of coastal environments.

BENOÎT LARROQUE received the Dipl.Ing. degree from the Ecole Nationale d'Ingénieurs ENIT, Tarbes, France, in 2004, and the Ph.D. degree in automatic control from the National Polytechnical Institute INP, Toulouse, France, in 2008. He is currently an Assistant Professor with the Université de Pau et des Pays de l'Adour, Anglet, France. His research is currently focused on remote lab technologies and supervision.